JACS
JOURNAL OF THE AMERICAN CHEMICAL SOCIETY
Article
pubs.acs.org/JACS

Liquid Crystal Reorientation Induced by Aptamer Conformational Changes

Patrick S. Noonan, Richard H. Roberts, and Daniel K. Schwartz*

Department of Chemical and Biological Engineering, University of Colorado Boulder, Boulder, Colorado 80309-0424, United States

Supporting Information

ABSTRACT: Aptamer-ligand binding events, involving small molecule targets, at a surfactant-laden aqueous/liquid crystal (LC) interface were found to trigger a LC reorientation that can be observed in real-time using polarized light. The response was both sensitive and selective: reorientation was observed at target concentrations on the order of the aptamer dissociation constant, but no response was observed in control experiments with target analogues. Circular dichroism and resonance energy transfer experiments suggested that the LC reorientation was due to a conformational change of the aptamer upon target binding. Specifically, under conditions where aptamer-ligand binding induced a conformational change from a relaxed random coil to more intricate secondary structures (e.g., double helix, G-quadruplex), a transition from planar to homeotropic LC orientation was observed. These observations suggest the potential for a label-free LC-based detection system that can simultaneously respond to the presence of both small molecules and nucleic acids.

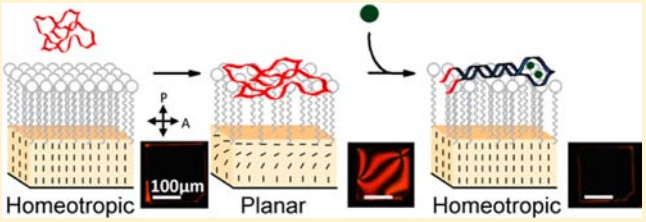

INTRODUCTION

The extraordinary physical properties of liquid crystal (LC) materials, long-range orientational order, responsiveness to external stimuli, and optical anisotropy, have made them uniquely valuable in display and optoelectronic applications. Recently, there is increasing momentum aimed at exploiting these same properties for other applications.[1] Of particular interest are applications where the LC responds to the presence of specific molecular compounds (e.g., for environmental monitoring or molecular diagnostic applications), translating these chemical signals into simple visual cues. Here, we demonstrate a dynamic LC response to specific binding events associated with what are arguably the ultimate molecular recognition elements, aptamers,[2,3] nucleic acid constructs that can be engineered to recognize a diverse range of targets. We define the mechanistic molecular principles underlying this response, specifically that the LC is influenced by the conformational change of the aptamer's secondary structure that occurs upon target binding.

As compared to standard methods based on monoclonal antibodies, the development of new aptamers[4−6] (using Systematic Evolution of Ligands by Exponential Enrichment [SELEX][3]) is faster, simpler, more robust, and yields aptamers that can bind selectively and with excellent sensitivity to a wide variety of targets, including small organic molecules,[7] proteins,[8,9] antibodies,[10] and even cells.[11] Coupled with an appropriate transduction method, aptamers could be the basis of a universal multiplexed detection strategy capable of the simultaneous detection of many different classes of analytes in the same sample.

The advantageous properties of aptamers as a molecular recognition element have inspired the development of biosensors capable of detecting aptamer-ligand binding events.[4−6] Significant progress has been made in the development of colorometric,[12−15] electrochemical,[16−18] fluorescence,[12,19,20] and mass-sensitive[21−23] strategies; however, the transduction strategies employed in these applications are fundamentally limited for multiplexed applications. When aptamer-ligand binding occurs in the bulk phase (e.g., nanoparticle colorometric and label-free fluorescence assays), a characteristic detection signal for each target species is required (e.g., fluorescence emission wavelength), placing a finite constraint on multiplexing capacity. Other strategies, such as mass-sensitive and electrochemical detection, confine the aptamer-ligand binding to an interface and thus have the potential for site-dependent multiplexing. However, signal transduction in many of these approaches is highly nonspecific (e.g., surface adsorption or localization of redox species), and the presence of even small amounts of interfering species will produce a false response. To achieve a universally multiplexed aptasensor, the transduction element should ideally be label-free and respond specifically to aptamer-ligand binding.

LC-based sensing schemes have proven capable of specific signal transduction through LC reorientations driven by interfacial enzymatic reactions[24] or molecular binding[25] events. The unique interfacial phenomena that lead to LC reorientation in these systems are complex and subtle, often involving the competition between multiple noncovalent

Received: January 18, 2013
Published: March 19, 2013

   dx.doi.org/10.1021/ja400619k | J. Am. Chem. Soc. 2013, 135, 5183−5189

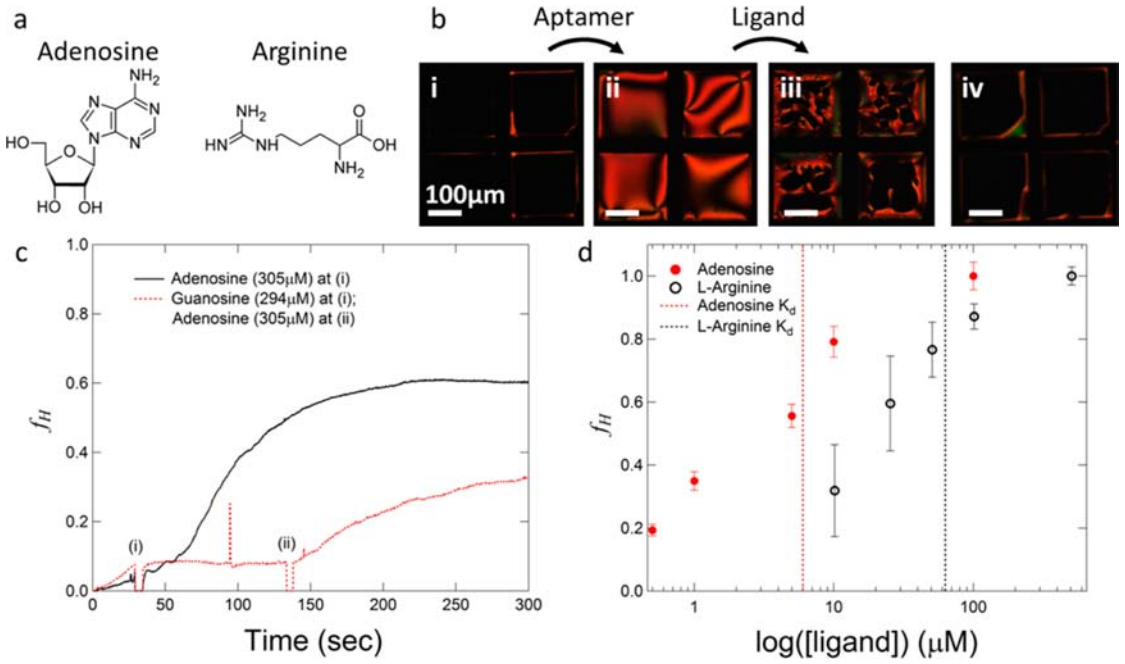

Figure 1. (a) Chemical structure of the aptamer targets. (b) Polarized light microscopy images of the aqueous/LC interface (i) laden with OTAB, (ii) after adsorption of the adenosine aptamer (2.5 μM), (iii) ∼20 s after addition of adenosine (∼300 μM), and (iv) ∼5 min after addition of adenosine; the same qualitative response is observed when using the arginine aptamer (Figure S1; [arginine aptamer] = 2.5 μM, [arginine] ≈ 1 mM). (c) Dynamic LC response upon addition of ligands; f_H: fractional increase in homeotropic area; the same qualitative response was observed when using the arginine aptamer (Figure S4). (d) f_H upon subsequent additions of either adenosine or arginine.

intermolecular interactions.[26] Understanding the underlying mechanisms behind these phenomena is of significant fundamental interest. Furthermore, the intrinsic cooperative behavior associated with the long-range orientational order of the LC phase provides a natural amplification effect, eliminating the need for (bio)chemical amplification, labeling, and/or expensive instrumentation. LC-based detection of aptamer binding would provide a potential path forward for label-free multiplexed unamplified detection of multiple target types (e.g., small molecules, nucleic acids, and proteins). The simultaneous detection of multiple molecular species in a label-free sensor scheme is an important goal, with widespread applications in areas including environmental monitoring, bio/chemical warfare detection, and medical diagnostics. Here, we demonstrate the underlying principles that will enable these applications.

In previous work, we developed a system where DNA hybridization at a surfactant-laden aqueous/LC interface caused a dynamic LC reorientation.[27,28] This approach exploited a LC anchoring transition from planar to homeotropic orientation caused by increasing surface concentrations of long-chain surfactants.[29] Upon adsorption of ssDNA to a surfactant-laden aqueous/LC interface (with homeotropic LC anchoring), the proximity of hydrophobic nucleobases to the hydrophobic LC perturbed the interfacial structure of the surfactant monolayer, causing LC reorientation to a planar configuration. Upon subsequent DNA hybridization, however, the DNA became less hydrophobic, allowing for a return to the interfacial structure associated with homeotropic anchoring. Thus, the orientation of the LC phase responded directly to a change in DNA conformation, in particular, a reduction in the amount of exposed hydrophobic nucleobases.

We hypothesized that a related approach could be used to detect other binding events associated with a nucleic acid conformational change at the aqueous/LC interface. Specifically, we utilized aptamers that are known to bind to the small molecule targets adenosine and arginine.[7,30] We chose these aptamers as representative examples because they represent a DNA (adenosine) and RNA (arginine) aptamer, their target molecules possess significantly different structures, and they demonstrate relatively predictable conformational changes upon binding to their target. For instance, structural studies[31,32] suggest that, in the absence of target, both aptamers have a significant portion of their nucleobases exposed, a conformation required for a LC orientational transition upon adsorption at the aqueous/LC interface. As the adenosine aptamer binds to its target, it folds into a conformation with Watson−Crick base pairing at its tails and a G-quadruplex structure at its head.[31] Similarly, the arginine aptamer is known to contain nucleobases within the core of the aptamer-ligand complex upon binding.[32] In both cases, ligand binding induces a significant decrease in the amount of exposed nucleobases, a conformational change analogous to that of DNA hybridization. Our aims in the current study were (i) to test the hypothesis that aptamer-ligand binding at an aqueous/LC interface can result in a LC reorientation and (ii) to verify and examine the relationship between the nucleic acid conformational changes that occur and an ability to induce a LC reorientation.

RESULTS AND DISCUSSION

Under the appropriate aqueous and interfacial conditions, we have, in fact, demonstrated the capability for aptamer-ligand binding events to induce a LC reorientation. When a sufficiently high surface concentration of cationic octadecyltrimethylammoniumbromide (OTAB) surfactant was adsorbed at an aqueous/LC interface,[27,28] the LC orientation was homeotropic as expected (Figure 1b(i)). Upon adsorption of aptamer (either the adenosine- or the arginine-specific

dx.doi.org/10.1021/ja400619k | J. Am. Chem. Soc. 2013, 135, 5183−5189

aptamer) to the OTAB laden aqueous/LC interface, a transition to tilted/planar LC orientation (Figure 1b(ii)) occurred, consistent with previous reports of the LC reorientation upon adsorption of unstructured ssDNA under similar conditions. This reorientation suggests that, under these aqueous conditions, the interfacial structures of both aptamers exhibited substantial ssDNA character (i.e., with exposed hydrophobic nucleobases). When the appropriate target was subsequently added, the reverse LC reorientation occurred, characterized by the nucleation and growth of small homeotropic domains (Figure 1b(iii)) that eventually coalesced to give a consistent homeotropic orientation (Figure 1b(iv)). This LC response mimicked the LC response upon DNA hybridization under the same interfacial conditions, suggesting that the conformational changes that occurred were also analogous.

Several control experiments were performed to demonstrate the specificity of the LC response to aptamer binding. The LC response upon addition of cytidine, thymidine, and guanosine 5′ monophosphate (GMP) to an adenosine aptamer laden interface, and upon addition of citrulline to an arginine aptamer laden interface, was tested (Figure S2). Furthermore, the LC response upon addition of adenosine to an interface laden with an adenosine aptamer containing a single base mismatch[31] was also tested. In all of these control experiments, no LC reorientation was observed (e.g., Figure S3) under the appropriate aqueous conditions (2.5 mM Na_2PO_4H, pH = 7.3, Supporting Information). To further illustrate this point, we measured the time dependence of the increase in fractional homeotropic area (f_H) extracted from polarized light microscopy images, providing a quantitative signature of the LC reorientation (Figure 1c, Figure S4). In these experiments, the addition of the appropriate aptamer consistently induced a transition to tilted/planar orientation. When adenosine or arginine was added ~30 s after stabilization of the planar LC orientation (t_i), a distinctive increase in homeotropic coverage was observed over the following several minutes (solid black curves in Figures 1c and S4). If GMP or citrulline was instead added at t_i, no increase in the homeotropic coverage was observed (dotted red curves in Figures 1c and S4) until adenosine or arginine was subsequently added. These experiments demonstrated specificity consistent with the requirements for multiplexed detection, as a target-specific LC reorientation occurred in the presence of interfering ligands with structures very similar to the target.

The sensitivity and quantitative nature of the LC response was tested by "dose-response" experiments (Figure 1d). Small amounts of adenosine or arginine were added to the aqueous phase after adsorption of the appropriate aptamer at an OTAB laden aqueous/LC interface; polarized light microscopy images were obtained upon stabilization of the LC orientation. A LC reorientation, characteristic of the specific response described above, was observed at bulk concentrations consistent with previously reported dissociation constants for aptamer-ligand binding[7,30] (dashed lines in Figure 1d). This systematic increase in homeotropic coverage observed with increasing concentrations of ligand provided a direct correlation between the LC reorientation and aptamer-ligand complex formation.

The operating conditions used in the experiments described above involved a relatively low ionic strength ($[Na_2PO_4H] \approx$ 2.5 mM). Under these conditions, we consistently observed a significant increase in the planar LC area upon adsorption of either aptamer (Figure 2a,c; Table 1) and a subsequent increase

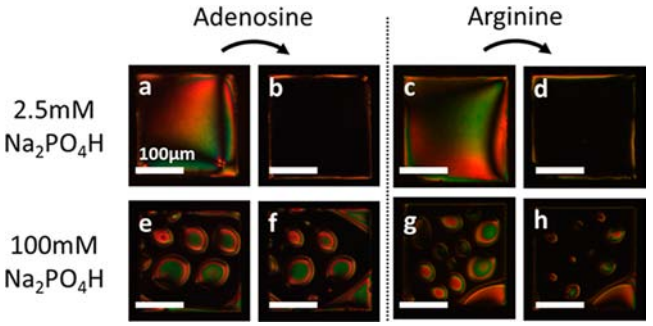

Figure 2. LC response at varying ionic strength: Polarized light microscopy images of the OTAB-laden aqueous/LC interface (a,c,e,g) after aptamer adsorption, or (b,d,f,h) ~3 min after subsequent addition of the appropriate ligand.

Table 1. Fractional Increase in Planar Area upon Addition of Aptamer, f_P; and Fractional Increase in Homeotropic Area upon Addition of Appropriate Ligand, f_H

aptamer	$[Na_2PO_4H]$ (mM)	f_P	f_H
adenosine	2.5	0.91 ± 0.10	0.88 ± 0.38
	100	0.37 ± 0.10	0.15 ± 0.07
arginine	2.5	0.47 ± 0.09	0.66 ± 0.10
	100	0.14 ± 0.14	0.50 ± 0.39

in the homeotropic area upon aptamer-ligand binding (Figure 2b,d; Table 1). However, at higher ionic strength ($[Na_2PO_4H] \approx$ 100 mM), we expected that changes in the interfacial environment and the bulk nucleic acid conformation would affect the ability to achieve LC orientational transitions. While others have observed LC ordering transitions with increased ionic strength, due to the formation of electric double layers[33] or interactions between the LC and chaotropic anions,[34] the conditions in our system are outside of the regime where these phenomena occur. Instead, we expected that increased ionic strength in the bulk aqueous phase would screen electrostatic interactions between the cationic head groups of the surfactant adsorbed at the aqueous/LC interface, allowing them to pack more tightly.[29] Perhaps more importantly, a similar electrostatic screening of the anionic DNA backbone at high ionic strength promotes DNA folding into a tightly wound random coil or, if the sequence permits it, a hairpin like structure.[35] Both of these phenomena inhibit the ability for the nucleobases of unbound aptamers to interact with the LC subphase and perturb the OTAB surface coverage. Consequently, we expected a decreased LC response to unbound aptamer adsorption under conditions of higher ionic strength. We observed that, for the adenosine and arginine aptamers, the fractional increase in planar area, f_P, indeed decreased at higher ionic strength (Figure 2e,g; Table 1).

We also hypothesized that the subsequent LC reorientation upon aptamer-ligand binding relied on a significant decrease in the hydrophobicity of the adsorbed nucleic acid.[28] However, a conformational change from a tightly wound random coil or hairpin structure may not involve a sufficiently dramatic change in nucleobase exposure to perturb the competitive balance for adsorption sites between DNA and OTAB. In fact, we observed that, at high ionic strength, ligand binding to the adenosine aptamer failed to induce a significant LC reorientation (Figure 2e,f), while ligand binding to the arginine aptamer revealed a qualitatively similar response to that observed at lower ionic strength (Figure 2g,h; Table 1). This suggested that, at

dx.doi.org/10.1021/ja400619k | J. Am. Chem. Soc. 2013, 135, 5183−5189

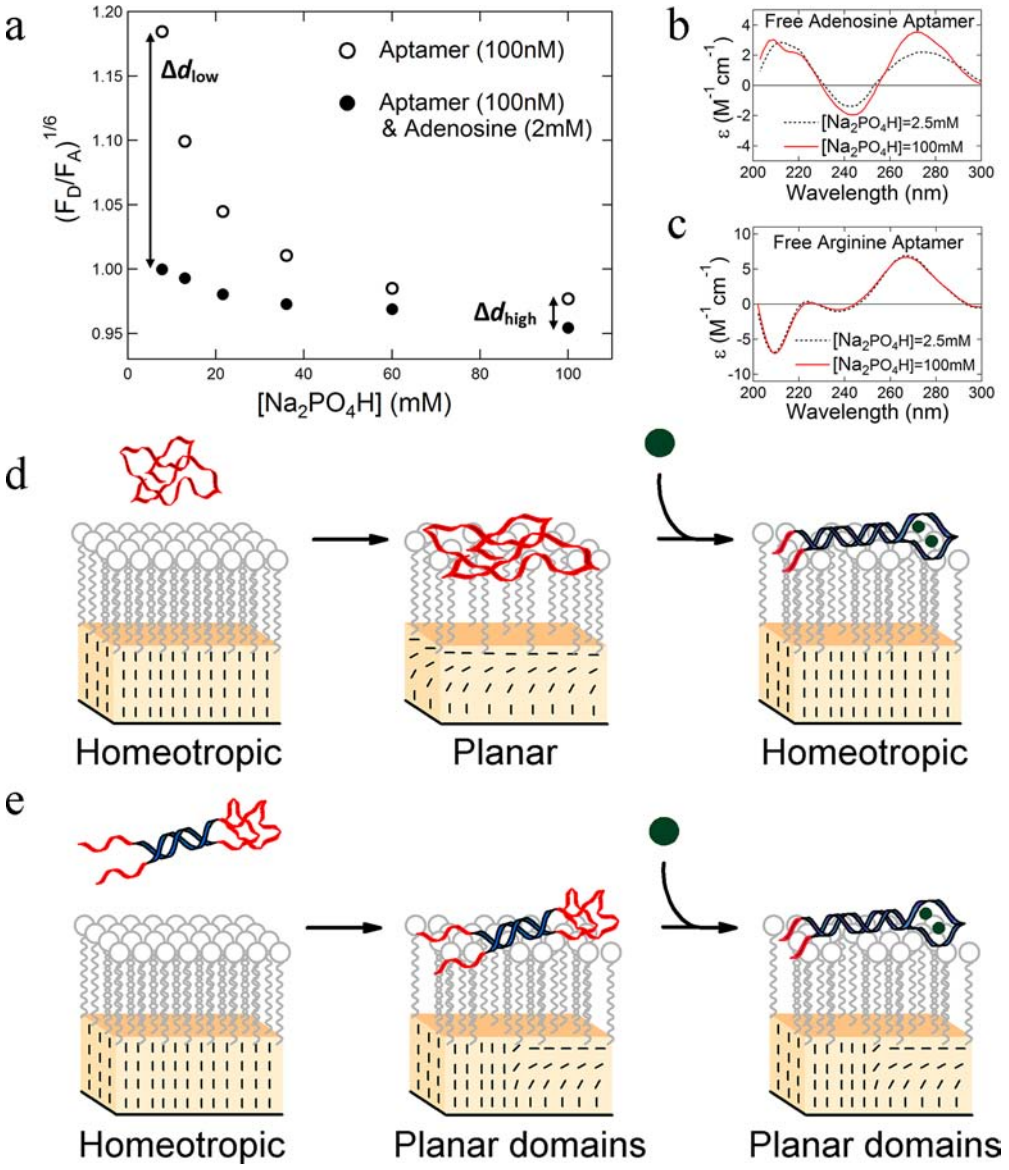

Figure 3. Aptamer structural studies: (a) Forster resonance energy transfer of a dual-labeled adenosine aptamer in bulk solution and at 25 °C; (b) circular dichroism (CD) spectra of 10 μM free adenosine aptamer in bulk solution; (c) CD spectra of 10 μM free arginine aptamer in bulk solution; and (d,e) schematic of the proposed mechanism for aptamer adsorption and binding at an OTAB laden aqueous/LC interface: (d) the arginine aptamer at low and high [ion], the adenosine aptamer at low [ion], and (e) the adenosine aptamer at high [ion]; note that schematics are not drawn to scale.

$[Na_2PO_4H] \approx 100$ mM, the conformational change of the adenosine aptamer upon ligand binding involved an insignificant change in nucleobase exposure, as we would expect if the free adenosine aptamer was already in a folded (e.g., hairpin) conformation prior to ligand binding. Conversely, ligand binding to the arginine aptamer still involved significant changes in nucleobase exposure at high ionic strengths, suggesting the free arginine aptamer was in a coil conformation at the increased ionic strength tested. Our structural studies, described below, are consistent with this model.

Solution phase Förster resonance energy transfer (FRET) measurements of a dual-labeled adenosine aptamer and solution phase circular dichroism (CD) spectroscopy provided the basis for these structural studies. With increasing ionic strength, the relative end-to-end distance d (calculated from FRET measurements as described in the Experimental Methods) decreased for both free and bound aptamer due to increased electrostatic screening (Figure 3a), as expected; however, this decrease was much more dramatic for the aptamer in the absence of ligand. Based on the model described above, we expected a large difference in the end-to-end distance (Δd_{low}) between the free and bound aptamer at low ionic strength (i.e., dramatic conformational change) and a significantly smaller difference (Δd_{high}) at high ionic strength (i.e., subtle conformational change). Consistent with these expectations, we found experimentally that $\Delta d_{low} \gg \Delta d_{high}$.

Short end-to-end distances of nucleic acids are indicative of either a tightly packed globular coil state or a hairpin-like structure. While FRET measurements cannot distinguish between these two states, we can make inferences based on the known conformations of the adenosine-aptamer ligand complex. Past studies have shown that the adenosine aptamer forms a highly folded aptamer-ligand complex where the 5′ and 3′ tails of the DNA are adjacent, analogous to a hairpin

dx.doi.org/10.1021/ja400619k | J. Am. Chem. Soc. 2013, 135, 5183−5189

conformation.[31] Under the plausible assumption that the aptamer-ligand complex at low ionic strength was in such a configuration, we conclude that the free aptamer at high ionic strength was also in a hairpin conformation, because d for this free aptamer was within 3% of that for the bound aptamer at low ionic strength.

CD spectroscopy measurements further elucidated the aptamer conformations. The formation of hairpin like structures in nucleic acids results in characteristic CD spectral shifts, while a transition from a loose random coil to a more compact globular structure is not expected to induce significant spectral shifts (Supporting Information).[36] The CD spectra of the free adenosine aptamer revealed spectral shifts at increased ionic strength (Figure 3b), consistent with hairpin formation, providing further evidence that the inability for ligand binding to induce a LC reorientation at increased ionic strength was related to an insignificant change in nucleobase exposure. Furthermore, the CD spectra of the free arginine aptamer were unvarying at high and low ionic strength (Figure 3c), indicative of a coil structure in both cases. This was consistent with a significant change in nucleobase exposure upon ligand binding (and the associated LC reorientation) at all ionic strengths measured. We also measured the CD spectra following addition of the appropriate ligand (Figure S5) at concentrations $\sim 10K_d$, and observed spectral shifts indicative of conformational changes consistent with those reported in the literature,[31,32] providing evidence that ligand binding occurred for both aptamers at both ionic strengths tested.

A mechanistic summary is schematically presented in Figure 3d and e. When the free aptamer is in a random coil conformation (Figure 3d, as for the adenosine aptamer at low ionic strength or the arginine aptamer at both low and high ionic strength), with exposed nucleobases, adsorption to the surfactant laden aqueous/LC interface results in an association between the exposed nucleobases and the LC subphase, via hydrophobic interactions, inducing a transition to planar/tilted LC orientation, as described previously.[28] Subsequent addition of the appropriate ligand results in a dramatic reduction in nucleobase exposure due to the formation of a highly folded aptamer-ligand complex, inducing the previously described transition to homeotropic orientation. Conversely, when the free aptamer is already in a folded conformation (e.g., a hairpin structure, Figure 3e), with few exposed nucleobases (the adenosine aptamer at high ionic strength), adsorption to the surfactant-laden aqueous/LC interface fails to cause a strong transition to planar LC orientation. Subsequent addition of the appropriate ligand may induce the formation of some intricate tertiary structures (e.g., G-quadruplex), but because the aptamer transitions from a weakly folded hairpin to these tertiary structures, there is little change in the amount of exposed hydrophobic bases. Consequently, there is a negligible change in the competitive balance between the DNA and the interfacial OTAB for adsorption sites, and the LC orientation is unaffected by the addition of ligand in this case.

CONCLUSION

The phenomena described here establish mechanistic principles sufficient to guide the development of LC-based aptasensing while also contributing to a fundamental understanding of LC anchoring. The underlying mechanisms of LC anchoring are complex and potentially involve a range of noncovalent interactions including electrostatic,[37] coordination,[38] and steric[39] effects. In the current study, we find that a deviation from a homeotropic LC anchoring state, associated with the interdigitation of the calamitic LC between surface bound alkyl surfactants,[28,40] occurred when an amphiphilic polymer (i.e., single-stranded nucleic acid) effectively competed with these surfactants for adsorption sites. We provide a direct relationship between the amphiphilic nature (i.e., nucleobase exposure) of the adsorbed nucleic acid and the LC anchoring. A previous study from our group provided evidence consistent with this mechanism,[28] but the direct relationship between nucleic acid structure and the LC anchoring presented here advances our understanding of how relatively subtle changes in amphiphilic adsorbates can induce LC reorientations. By employing this broadly applicable and controllable conformational change in a surface bound species to induce a predictable LC anchoring transition, we illustrate the potential for highly multiplexed aptasensing applications.

This aptasensing scheme is label-free and has successfully utilized LCs as a transduction element that responds specifically to conformational changes in the aptamer upon ligand binding, fulfilling the fundamental requirements for a highly multiplexed aptasensor. Importantly, the nonspecific adsorption of free aptamer did not induce a false-positive, but in fact promoted a negative response (planar LC orientation). As described above, this is not the case in many other aptasensing strategies, forcing them to rely on efficient rinsing of nonspecifically adsorbed species, a technique that is infeasible for highly multiplexed applications. Moreover, with our approach, multiplexed detection of aptamer targets can be readily combined with simultaneous detection of nucleic acid targets via hybridization.[27] Realization of an actual LC-based aptasensor device will require a demonstration of performance in complex media and employing microstructured substrates as a LC sensing platform, an area in which our lab[39] and others[41−43] have made significant progress. While our results at varying ionic strength may suggest that some aptamers are more limited than others in terms of their ability to function under diverse conditions, tweaking the interfacial conditions, such as surface charge density and surfactant composition,[43] will allow for the rational design of arrays for the simultaneous detection of a range of aptamer targets in a complex media (e.g., wastewater, serum, etc.). Using this type of rational design and the molecular understanding of the LC reorientation achieved here, our future work will involve extending the scope of our approach toward a detection platform capable of label-free simultaneous multi-species detection.

EXPERIMENTAL METHODS

Preparation of self-assembled monolayers (SAMs) of octadecyltriethoxysilane (OTES) (Gelest Inc.) was completed according to published procedures.[44] Soda lime glass microscope slides (Corning Inc.) were cleaned sequentially with 2% aqueous micro-90, deionized water (18.2 MΩ), and piranha solution (30% aqueous H_2O_2 (Fisher Scientific) and concentrated H_2SO_4 (Fisher Scientific) 1:3, v/v) at ∼80 °C for 1 h. (Caution: Piranha reacts strongly with organic compounds and should be handled with extreme caution; do not store in a closed container.) Following piranha cleaning, microscope slides were rinsed with deionized water (18.2 MΩ) and dried under a stream of ultrapure N_2. A deposition solution of *n*-butylamine (Fisher Scientific) and OTES was prepared in toluene (Fisher Scientific) at 1:3:200 volumetric ratios, respectively, and warmed to 60 °C. The clean and dry microscope slides were then rinsed with toluene, submerged in the warm deposition solution, and incubated for 1 h at 60 °C. Upon removal from the deposition solution, the slides were rinsed with toluene, dried under a stream of ultrapure N_2, and stored

dx.doi.org/10.1021/ja400619k | J. Am. Chem. Soc. 2013, 135, 5183−5189

at room temperature in a vacuum desiccator. A custom-built contact angle goniometer was used to verify that the water contact angle (θ_C, measured via the static sessile drop method) of the prepared SAMs was sufficient to indicate strong homeotropic anchoring ($\theta_C > 95°$).

OTAB (Sigma-Aldrich)-laden LC films were prepared by housing the nematic E7 LC (Merck KGaA) within the pores of an electron microscopy grid (Electron Microscopy Sciences) placed onto a solid glass substrate functionalized with an octadecyltriethoxysilane self-assembled monolayer (SAM).[44] The SAM maintained homeotropic orientation of the LC at the solid substrate. The grids were contained within silicone isolators (Grace-bio Laboratories, #664206) placed onto SAM-functionalized glass. A solution of OTAB in E7 was prepared at [OTAB] ≈ 100 μM. The pores of the electron microscopy grid were then filled with the LC/OTAB mixture by pipetting ∼250 nL into the grid and removing the excess via capillary action. Next, the wells were filled with ∼25 μL of an aqueous solution (2.5 mM Na_2PO_4H; Sigma Aldrich). The ssDNA adenosine aptamer (5′ACCTGGGGGAGTATTGCGGAGGAAGGT3′; Invitrogen), a ssDNA mismatch adenosine aptamer (5′ACCTGGGGGAG-TATTGCGGAGCAAGGT3′; Invitrogen), or the ssRNA arginine aptamer (5′GACGAGAAGGAGCGCUGGUUCUACUAGCAG-GUAGGUCACUCGUC3′; Biosearch Technologies) were added by pipetting small volumes (1−2 μL) of high concentration stocks (∼100 μM in dH_2O) into the aqueous phase to achieve a final [aptamer] ≈ 2.5 μM. Subsequent addition of the appropriate ligand (adenosine, GMP, cytidine, thymidine, L-arginine, L-citruline; Sigma-Aldrich) was also performed by pipetting small volumes (1−2 μL) of high concentration stocks (∼11−17 mM in dH_2O) into the aqueous phase. The LC orientation and textures were observed between crossed polarizers with an Olympus microscope (model BH2-UMA) modified for transmission mode.

The relative end-to-end distance of dual-labeled adenosine aptamer (FAM-5′ACCTGGGGGAGTATTGCGGAGGAAGGT3′-TAMRA, Biosearch Technologies) was measured using Förster resonance energy transfer (FRET) spectroscopy. The dual-labeled aptamer (100nM) was constituted in buffer at varying ionic strength ([Na_2PO_4H] ≈ 7.8−100 mM) in the absence and presence (2 mM) of adenosine. Using a fluorescence plate reader (Wallac 1420 VICTOR,[2] Perkin-Elmer), we excited the dual-labeled aptamer at λ_{ex} = 485 nm and measured the emission intensity at $\lambda_{d,em}$ = 528 nm (F_D, donor emission intensity) and $\lambda_{a,em}$ = 585 nm (F_A, acceptor emission intensity). We used these intensities to determine the relative distance between fluorophores according to eq 1:

$$d = \left(\frac{F_D}{F_A}\right)^{1/6} \quad (1)$$

This equation is simplified from an equation that defines the absolute distance between fluorophores.[45] In our studies, this relative comparison of the distance between fluorophores is sufficient to make inferences about the nucleic acid conformations. Because our FRET pair is tethered on opposing ends of the DNA strand, this relative separation between fluorophores is directly proportional to the relative end-to-end distance of the DNA.

Circular dichroism spectroscopy (Chirascan-plus CD spectrometer, Applied Photophysics) was used to probe the conformational changes that occur with varying ionic strength and upon addition of ligands. Either the adenosine or the arginine aptamer was constituted in 2.5 mM or 100 mM aqueous Na_2PO_4H at 10 μM to a total volume of 300 μL. After the CD spectra were measured in the absence of ligand, 30 μL of a concentrated ligand stock ([adenosine] ≈ 600 μM, [arginine] ≈ 6600 μM) was added directly to the sample cuvette and mixed via pipetting to achieve a [ligand] ≈ 10*K_d for both aptamers. We also measured the CD spectra of pure buffer at [Na_2PO_4H] ≈ 2.5 and 100 mM, as well as adenosine and arginine in the absence of aptamer under both of these buffer conditions. The data obtained were reported in terms of ellipticity (θ). After subtracting the buffer baseline, we converted θ to molar circular dichroism ($\Delta\varepsilon$) according to eq 2:

$$\Delta\varepsilon = \frac{\theta/32.982}{C \times l} \quad (2)$$

where C is the concentration of nucleic acid in moles of nucleobases and l is the optical path-length. Finally, we subtracted the ligand contribution to $\Delta\varepsilon$ on a per mole basis and applied the Savitzy−Golay algorithm to smooth the resulting CD spectra.

■ ASSOCIATED CONTENT

Supporting Information

Polarized light micrographs, chemical structures, dynamic response data, and circular dichroism spectra, as well as a brief discussion regarding image analysis, LC response sensitivity, and CD spectroscopy analysis. This material is available free of charge via the Internet at http://pubs.acs.org.

■ AUTHOR INFORMATION

Corresponding Author

daniel.schwartz@colorado.edu

Notes

The authors declare no competing financial interest.

■ ACKNOWLEDGMENTS

This work was supported by the National Science Foundation (Award #CBET-1160202) and the Liquid Crystal Materials Research Center (NSF/MRSEC, Award No. DMR-820579).

■ REFERENCES

(1) Lowe, A. M.; Abbott, N. L. *Chem. Mater.* **2012**, *24*, 746−758.
(2) Ellington, A. D.; Szostak, J. W. *Nature* **1990**, *346*, 818−822.
(3) Tuerk, C.; Gold, L. *Science* **1990**, *249*, 505−510.
(4) Cho, E. J.; Lee, J. W.; Ellington, A. D. *Annu. Rev. Anal. Chem.* **2009**, *2*, 241−264.
(5) Song, S. P.; Wang, L. H.; Li, J.; Zhao, J. L.; Fan, C. H. *TrAC, Trends Anal. Chem.* **2008**, *27*, 108−117.
(6) Iliuk, A. B.; Hu, L.; Tao, W. A. *Anal. Chem.* **2011**, *83*, 4440−4452.
(7) Huizenga, D. E.; Szostak, J. W. *Biochemistry* **1995**, *34*, 656−665.
(8) Bock, L. C.; Griffin, L. C.; Latham, J. A.; Vermaas, E. H.; Toole, J. J. *Nature* **1992**, *355*, 564−566.
(9) Green, L. S.; Jellinek, D.; Jenison, R.; Ostman, A.; Heldin, C.-H.; Janjic, N. *Biochemistry* **1996**, *35*, 14413−14424.
(10) Miyakawa, S.; Nomura, Y.; Sakamoto, T.; Yamaguchi, Y.; Kato, K.; Yamazaki, S.; Nakamura, Y. *RNA* **2008**, *14*, 1154−1163.
(11) Sefah, K.; Tang, Z. W.; Shangguan, D. H.; Chen, H.; Lopez-Colon, D.; Li, Y.; Parekh, P.; Martin, J.; Meng, L.; Phillips, J. A.; Kim, Y. M.; Tan, W. H. *Leukemia* **2009**, *23*, 235−244.
(12) Li, B.; Dong, S.; Wang, E. *Chem.-Asian J.* **2010**, *5*, 1262−1272.
(13) Liu, J. W.; Lu, Y. *Angew. Chem., Int. Ed.* **2006**, *45*, 90−94.
(14) Xiang, Y.; Lu, Y. *Nat. Chem.* **2011**, *3*, 697−703.
(15) Zhao, W.; Chiuman, W.; Lam, J. C. F.; McManus, S. A.; Chen, W.; Cui, Y.; Pelton, R.; Brook, M. A.; Li, Y. *J. Am. Chem. Soc.* **2008**, *130*, 3610−3618.
(16) Du, Y.; Chen, C.; Zhou, M.; Dong, S.; Wang, E. *Anal. Chem.* **2011**, *83*, 1523−1529.
(17) Lai, R. Y.; Plaxco, K. W.; Heeger, A. J. *Anal. Chem.* **2006**, *79*, 229−233.
(18) Tang, D.; Tang, J.; Li, Q.; Su, B.; Chen, G. *Anal. Chem.* **2011**, *83*, 7255−7259.
(19) Tan, Y.; Zhang, X.; Xie, Y.; Zhao, R.; Tan, C.; Jiang, Y. *Analyst* **2012**, *137*, 2309−2312.
(20) Nutiu, R.; Li, Y. *J. Am. Chem. Soc.* **2003**, *125*, 4771−4778.
(21) Knudsen, S. M.; Lee, J.; Ellington, A. D.; Savran, C. A. *J. Am. Chem. Soc.* **2006**, *128*, 15936−15937.
(22) Li, Y.; Lee, H. J.; Corn, R. M. *Anal. Chem.* **2007**, *79*, 1082−1088.
(23) Wang, Q.; Huang, J.; Yang, X.; Wang, K.; He, L.; Li, X.; Xue, C. *Sens. Actuators, B* **2011**, *156*, 893−898.

(24) Park, J. S.; Teren, S.; Tepp, W. H.; Beebe, D. J.; Johnson, E. A.; Abbott, N. L. *Chem. Mater.* **2006**, *18*, 6147−6151.
(25) Brake, J. M.; Daschner, M. K.; Luk, Y. Y.; Abbott, N. L. *Science* **2003**, *302*, 2094−2097.
(26) Bai, Y.; Abbott, N. L. *Langmuir* **2011**, *27*, 5719−5738.
(27) Price, A. D.; Schwartz, D. K. *J. Am. Chem. Soc.* **2008**, *130*, 8188−8194.
(28) McUmber, A. C.; Noonan, P. S.; Schwartz, D. K. *Soft Matter* **2012**, *8*, 4335−4342.
(29) Brake, J. M.; Abbott, N. L. *Langmuir* **2002**, *18*, 6101−6109.
(30) Famulok, M. *J. Am. Chem. Soc.* **1994**, *116*, 1698−1706.
(31) Lin, C. H.; Patel, D. J. *Chem. Biol.* **1997**, *4*, 817−832.
(32) Yang, Y. S.; Kochoyan, M.; Burgstaller, P.; Westhof, E.; Famulok, M. *Science* **1996**, *272*, 1343−1347.
(33) Carlton, R. J.; Gupta, J. K.; Swift, C. L.; Abbott, N. L. *Langmuir* **2012**, *28*, 31−36.
(34) Carlton, R. J.; Ma, C. D.; Gupta, J. K.; Abbott, N. L. *Langmuir* **2012**, *28*, 12796−12805.
(35) Anderson, C. F.; Record, M. T. *Annu. Rev. Phys. Chem.* **1995**, *46*, 657−700.
(36) Kypr, J.; Kejnovska, I.; Renciuk, D.; Vorlickova, M. *Nucleic Acids Res.* **2009**, *37*, 1713−1725.
(37) Zou, J.; Bera, T.; Davis, A. A.; Liang, W.; Fang, J. *J. Phys. Chem. B* **2011**, *115*, 8970−8974.
(38) VanTreeck, H. J.; Most, D. R.; Grinwald, B. A.; Kupcho, K. A.; Sen, A.; Bonds, M. D.; Acharya, B. R. *Sens. Actuators, B* **2011**, *158*, 104−110.
(39) Noonan, P. S.; Shavit, A.; Acharya, B. R.; Schwartz, D. K. *ACS Appl. Mater. Interfaces* **2011**, *3*, 4374−4380.
(40) Abbott, N. L.; Brake, J. M.; Mezera, A. D. *Langmuir* **2003**, *19*, 6436−6442.
(41) Liu, Y.; Cheng, D.; Lin, I. H.; Abbott, N. L.; Jiang, H. *Lab Chip* **2012**, *12*, 3746−3753.
(42) Cheng, D. M.; Sridharamurthy, S. S.; Hunter, J. T.; Park, J. S.; Abbott, N. L.; Jiang, H. R. *J. Microelectromech. Syst.* **2009**, *18*, 973−982.
(43) Yang, Z. Q.; Gupta, J. K.; Kishimoto, K.; Shoji, Y.; Kato, T.; Abbott, N. L. *Adv. Funct. Mater.* **2010**, *20*, 2098−2106.
(44) Walba, D. M.; Liberko, C. A.; Korblova, E.; Farrow, M.; Furtak, T. E.; Chow, B. C.; Schwartz, D. K.; Freeman, A. S.; Douglas, K.; Williams, S. D.; Klittnick, A. F.; Clark, N. A. *Liq. Cryst.* **2004**, *31*, 481−489.
(45) Wu, P. G.; Brand, L. *Anal. Biochem.* **1994**, *218*, 1−13.